Nanoplatform based on carbon nanoparticles loaded with doxorubicin enhances apoptosis by generating reactive oxygen species for effective cancer therapy

YUSHENG LIU[1,2*], JUNFENG ZHANG[1*], CHUNYING WU[1], YIGUI LAI[1], HUIJIE FAN[1,2], QIANG WANG[1], ZHAOLIN LIN[1], JISHANG CHEN[1], XIAOSHAN ZHAO[1,2] and XUEFENG JIANG[1,2]

[1]Department of Traditional Chinese Medicine, Yangjiang People's Hospital, Yangjiang, Guangdong 529500, P.R. China; [2]College of Traditional Chinese Medicine, Southern Medical University, Guangzhou, Guangdong 510515, P.R. China

Received February 20, 2024; Accepted April 9, 2024

DOI: 10.3892/ol.2024.14421

Abstract. At present, due to its wide application and relatively low cost, chemotherapy remains a clinically important cancer treatment option; however, a number of chemotherapeutic drugs have important limitations, such as lack of specificity, high toxicity and side effects, and multi-drug resistance. The emergence of nanocarriers has removed numerous clinical application limitations of certain antitumor chemotherapy drugs and has been widely used in the treatment of tumors with nanodrugs. The present study used carbon nanoparticles (CNPs) as a nanocarrier for doxorubicin (DOX) to form the novel nanomedicine delivery system (CNPs@DOX)was demonstrated by UV-vis and fluorescence spectrophotometry, ζ potential and TEM characterization experiments. The results confirmed the successful preparation of CNPs@DOX nanoparticles with a particle size of 96±17 nm, a wide range of absorption and a negatively charged surface. Furthermore, CNPs@DOX produced more reactive oxygen species and induced apoptosis, and thus exhibited higher cytotoxicity than DOX, which is a small molecule anticancer drug without a nanocarrier delivery system.. The present study provides a strategy for the treatment of tumors with nanomedicine.

Introduction

Cancer is a worldwide public health issue and one of the major contributors to the global burden of disease (1). According to the Global Cancer Observatory 2020 database, ~10 million people worldwide die from cancer each year (2). Given the ageing population, the number of cancer deaths worldwide is expected to continue to rise, creating a significant public health burden (3,4). Current cancer treatment options include surgery, anticancer drugs, radiation therapy and immunotherapy, alone or in combination (5). Chemotherapy has been a clinically important cancer treatment option due to its wide application and relatively low cost. However, numerous chemotherapeutic drugs have important limitations, such as lack of specificity, toxic side effects, poor water solubility, low bioavailability and multi-drug resistance (6-8). For example, doxorubicin (DOX) is an antitumor chemotherapy drug that has been widely used in the clinic and has shown powerful therapeutic effects against several cancer types, including breast cancer (9), malignant lymphoma (10), acute leukemia (11) and lung cancer (12,13). However, due to the lack of tumor specificity and serious side effects, such as myelosuppression and cardiac toxicity, its clinical application is severely limited (14).

To solve the clinical problems of chemotherapy drugs, drug delivery systems based on nanocarriers have been widely developed, which have clear advantages in cancer therapy. Firstly, due to the enhanced permeability and retention (EPR) of the tumor, the nanosystem has an increased inherent capacity to accumulate at the tumor site rather than in normal tissue (15,16). Secondly, blood vessels in tumor tissue have a larger aperture compared with healthy tissue, leading to the preferential accumulation of nanodrugs in the tumor, improving the therapeutic effect and reducing systemic toxicity (17). At present, due to their excellent physical and chemical properties, rich functional groups (such as amino, hydroxyl and carboxyl groups), large surface area and good biocompatibility, carbon-based nanomaterials, including carbon nanoparticles, carbon nanotubes, graphene and its derivatives, have aroused great interest in biomedical applications such as drug delivery, bioimaging and therapy (18-20).

In present study, UV-vis and fluorescence spectrophotometry, ζ potential and TEM characterization experiments were used to verify whether the nanodrug delivery system was successfully prepared. Cytotoxicity assay, intracellular ROS detection and apoptosis assay were performed to evaluate the toxicity and killing mechanism of the nanomedicine delivery

Correspondence to: Dr Xuefeng Jiang, Department of Traditional Chinese Medicine, Yangjiang People's Hospital, 42 Dongshan Road, Jiangcheng, Yangjiang, Guangdong 529500, P.R. China
E-mail: 670621447@qq.com

*Contributed equally

Key words: carbon nanoparticles, doxorubicin, reactive oxygen species, apoptosis, cancer therapy

system on cancer cells. This study aims to provide a potential strategy for the therapy of tumors with nanomedicine.

Materials and methods

Materials. CNPs were synthesized based on a previously reported method (21). DOX was purchased from Merck KGaA. Other chemical reagents for the experiment were bought from Sinopharm Chemical Reagent Co., Ltd., unless otherwise specified.

Material synthesis. CNPs were prepared using heat treatment. In brief, the carbon source [citric acid, 20% (w/v)] and the surface modifier [reduced glutathione (GSH), 20% (w/v)] were dissolved in deionized water and heated in an oil bath (130˚C) for 10 min. After the reaction, the solution was cooled to room temperature and the pH was adjusted to 7.4. The solution was then further dialyzed using a dialysis bag [molecular weight cut-off (MWCO)=3,500 Da] to remove free citric acid and GSH. Finally, the solution was filtered to retain the liquid, and CNPs were obtained.

DOX solution (800 mg/l; 5 ml) was slowly added to the CNP solution at room temperature and magnetically stirred for 2 h. After the mixed solution was allowed to stand for 2 h, the free DOX was removed by dialysis through the dialysis bag (MWCO=14 kDa). The obtained CNPs@DOX was stored at room temperature for characterization and experimentation.

Characterization methods. A total of 10 μl CNP (100 mg/l) and CNPs@DOX (100 mg/l) solutions were dripped onto carbon-coated 400-mesh copper grids by pipette gun and air-dried for 24 h to prepare the sample for transmission electron microscopy (TEM; Hitachi, Ltd.) observation. The ζ potentials of aqueous CNPs and CNPs@DOX were measured using dynamic light scattering (Malvern Instruments, Ltd.). The ultraviolet (UV)-visible (vis) absorption and fluorescence spectra were measured using a UV spectrophotometer (Hitachi, Ltd.) and fluorescence spectrophotometer (Hitachi, Ltd.), respectively.

DOX loading study in CNPs@DOX. DOX solutions (300, 400, 500, 800 and 1,000 mg/l) were added to CNP (2,000 mg/l) solution to synthesize CNPs@DOX. By measuring the absorbance of DOX at 480 nm in aqueous solution, the standard calibration curve of DOX was obtained and the drug loading efficiency (DLE) of CNPs@DOX was calculated (22). The DLE was calculated as follows: DLE (%)=[(amount of DOX-amount of free DOX)/(amount of DOX)] x100.

Cell culture. Mouse breast cancer 4T1 and human breast cancer MCF7 cell lines were purchased from the Cell Bank of Chinese Academy of Sciences. DMEM and FBS were purchased from Gibco; Thermo Fisher Scientific, Inc. Cells were cultured using DMEM supplemented with 10% FBS (37˚C; 5% CO_2 atmosphere).

Cytotoxicity evaluation. The cytotoxicity of CNPs@DOX and DOX were evaluated using the 4T1 and MCF7 cell lines. The cells were seeded in 96-well plates ($5x10^3$ cells per well) and incubated in DMEM containing different concentrations (0, 0.1, 1, 2.5, 5 and 10 mg/l) of CNPs@DOX or DOX for 24 h at 37˚C. The original medium was aspirated and the cells were incubated for 1 h with fresh medium containing 10 μl Cell Counting Kit-8 reagent (Dojindo Laboratories, Inc.). Finally, the absorbance [optical density (OD)] was measured at 450 nm with a microplate reader to calculate cell viability as follows: Cell viability (%)=[($OD_{treated}$-OD_{blank})/($OD_{control}$-OD_{blank})] x100, where $OD_{treated}$, $OD_{control}$ and OD_{blank} were the absorbance values of the sample wells.

Cell apoptosis. The 4T1 cells were cultured in 6-well plates ($1x10^5$ cells per well) for 12 h at 37˚C, and when cell proliferation reached 60-70%, the original medium was sucked out and the cells continued to be cultured with fresh medium containing CNPs@DOX solution (5 mg/l DOX) and DOX solution (5 mg/l) for 24 h at 37˚C. The cells were then trypsinized, washed with PBS and collected ($1x10^6$ cells). An annexin V-FITC/PI Apoptosis detection Kit (BD Biosciences) was used to stain apoptotic cells by mixing 100 μl cell suspension, 5 μl annexin V-FITC and 5 μl PI. The cells were incubated for 15 min at 37˚C and 200 μl binding buffer (0.01 M HEPES, pH 7.4; 0.14 M NaCl; 2.50 mM $CaCl_2$) was added to each suspension. Finally, apoptosis was measured using a flow cytometer (FACSCalibur™; BD Biosciences) and analyzed by BD FACSDiva™ Software v9.0.

ROS detection in vitro. Intracellular ROS changes were detected using the fluorescent probe 2',7'-Dichlorodihydrofluorescein diacetate (DCFH-DA). Specifically, the 4T1 cells ($1x10^5$ cells) were cultured with media containing CNPs@DOX solution (2.5 mg/l DOX) and DOX solution (2.5 mg/l) for 24 h at 37˚C, and then incubated with the ROS Assay Kit (S0033S, Beyotime Biotechnology) according to the manufacturer's instructions. Finally, confocal laser scanning microscopy (CLSM; Olympus Corporation) was used to detect intracellular ROS production.

Statistical analysis. The data are expressed as the mean ± standard deviation. GraphPad Prism 8 software (Dotmatics) was used for statistical analysis. The unpaired t-test or one-way analysis of variance with Tukey's post hoc test was used to compare the differences between the experimental groups. Drug loading efficiency was calculated using a standard calibration curve. $P<0.05$ was considered to indicate a statistically significant difference.

Results and discussion

Characterization of CNPs@DOX. The particle sizes of CNPs and CNPs@DOX were assessed using TEM. The average particle size of CNPs in the aqueous solution was 79±14 nm, and the average particle size of CNPs combined with DOX to form the nanomedical drug delivery system CNPs@DOX was 96±17 nm. CNPs@DOX, as a nanomedicine, can target tumor tissue through the EPR effect, whereas DOX, as a small molecule drug, does not have this targeting ability. Therefore, CNPs@DOX is conducive to the accumulation of DOX at the tumor site through the EPR effect, thereby exerting antitumor effects (Fig. 1).

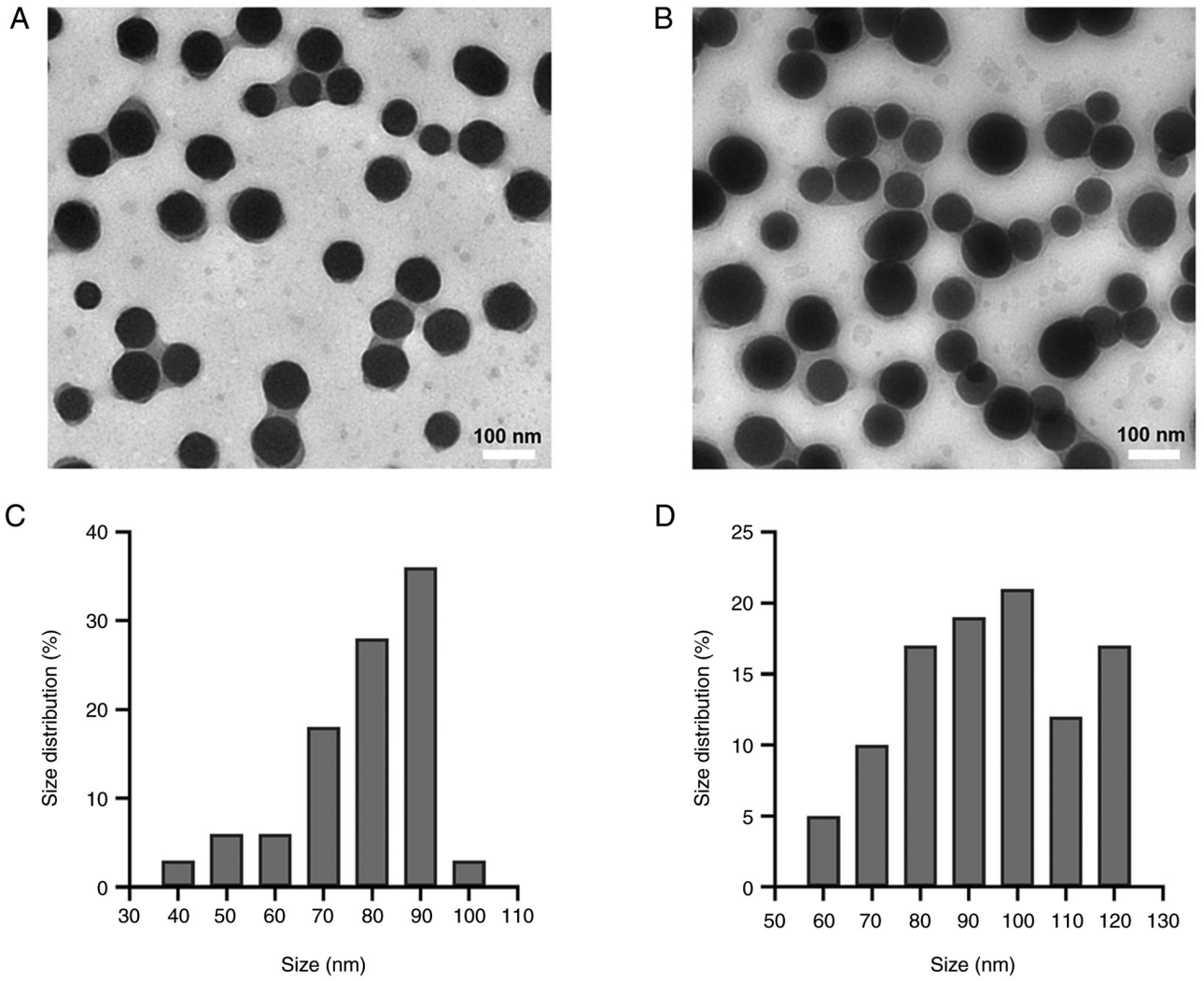

Figure 1. Material characterization. Transmission electron microscopy images of (A) CNPs and (B) CNPs@DOX. Particle size distribution of (C) CNPs and (D) CNPs@DOX. CNPs, carbon nanoparticles; DOX, doxorubicin.

UV-vis spectra demonstrated notable absorbance of CNPs at 374 nm and of DOX at 480 nm; however, CNPs@DOX demonstrated strong absorbance at 518 nm (Fig. 2A), which was different from that of both CNPs and DOX due to the interaction between the CNPs and the DOX. Moreover, fluorescence spectroscopy revealed an emission peak at 471 nm for CNPs, at 592 nm for DOX and at 468 nm for CNPs@DOX (Fig. 2B).

The ζ potential of the CNPs was ~-33.2 mV, and the introduction of DOX was associated with a marked increase in the ζ potential to ~-15.6 mV (Fig. 2C; Table I), which indicates the successful preparation of CNPs@DOX. It has been reported that the negative charge on the surface of nanoparticles makes them more conducive to travelling within blood circulation (23,24).

The aforementioned results confirmed successful preparation of CNPs@DOX nanoparticles with a particle size of 96±17 nm, a wide range of absorption and a negatively charged surface.

Table I. ζ potentials of CNPs and CNPs@DOX in aqueous solution.

Group	ζ potential, mV
CNPs	-33.2±4.3
CNPs@DOX	-15.6±3.5

Data are presented as the mean ± standard deviation. CNPs, carbon nanoparticles; DOX, doxorubicin.

DOX loading study in CNPs@DOX. To assess the DOX loading rate in CNPs@DOX, DOX solutions of different concentrations (300, 400, 500, 800 and 1,000 mg/l) were added to CNPs (2,000 mg/l) solution to synthesize CNPs@DOX. The DLE was calculated using standard calibration curves of DOX (Fig. S1). The results demonstrated that the DLE reached ≥77.52% when DOX solution was added at 800 mg/l (Fig. 2D). All experiments in the present study used CNPs@DOX, synthesized by adding 800 mg/l DOX solution (DLE=77.52%).

Cytotoxicity evaluation. The cytotoxicity assays of free DOX and CNPs@DOX demonstrated notable dose-dependent cell

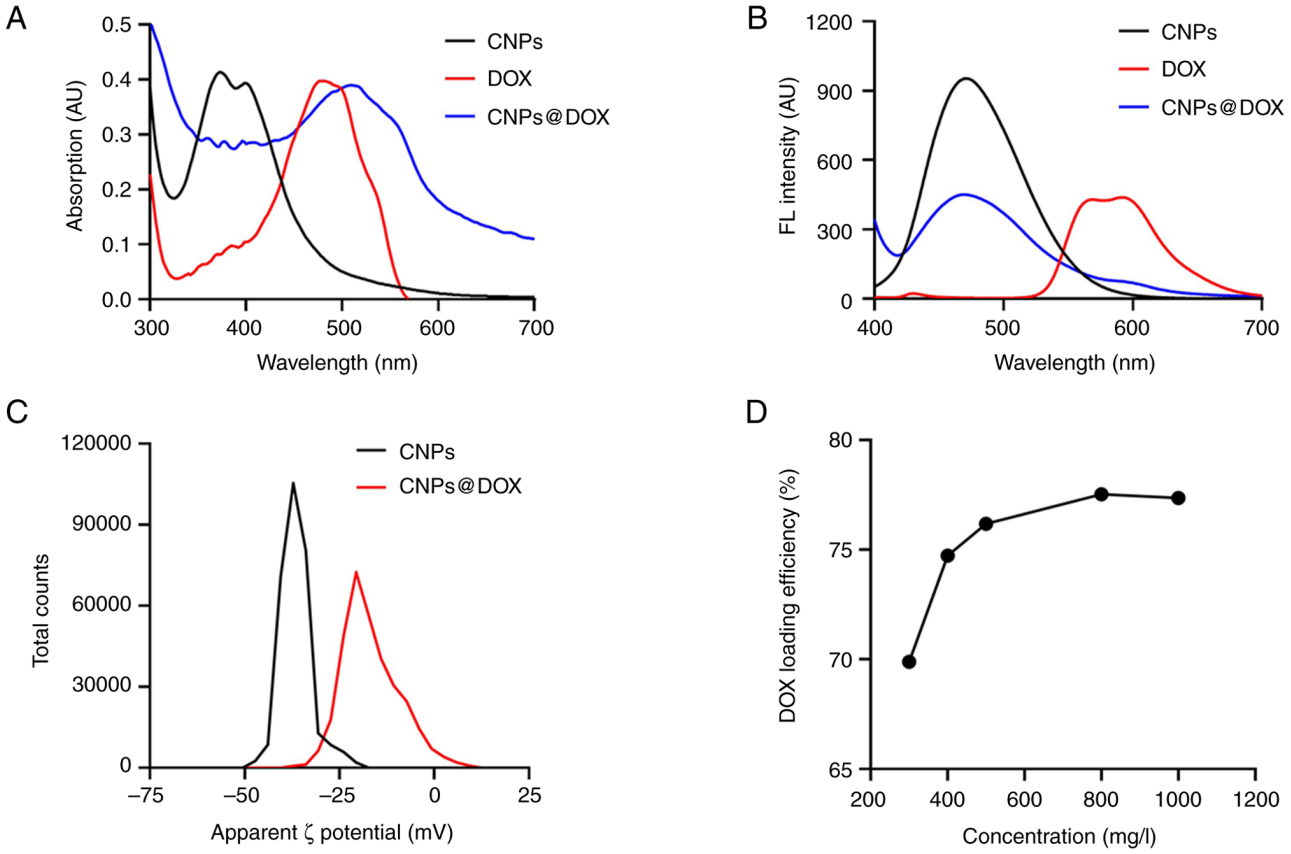

Figure 2. Material characterizations and drug loading efficiency. (A) Ultraviolet-visible spectra of CNPs, DOX and CNPs@DOX. (B) FL spectra of CNPs, DOX and CNPs@DOX. (C) ζ potentials of CNPs and CNPs@DOX in aqueous solution. (D) Drug loading efficiency of CNPs@DOX at different concentrations of DOX. CNPs, carbon nanoparticles; DOX, doxorubicin; FL, fluorescence.

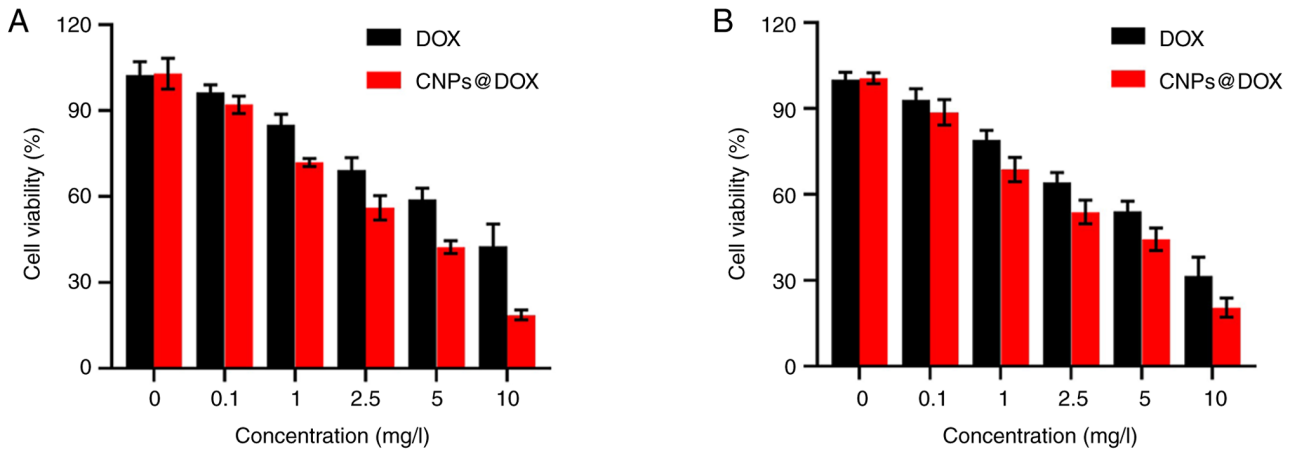

Figure 3. Cytotoxicity evaluation. Cytotoxicity after 24 h of (A) 4T1 and (B) MCF7 cells incubated with DOX and CNPs@DOX at different concentrations (0, 0.1, 1, 2.5, 5 and 10 mg/l). CNPs, carbon nanoparticles; DOX, doxorubicin.

viability inhibition in both the 4T1 and MCF7 cells at 24 h (Fig. 3). In particular, when the drug concentration was 5 or 10 mg/l, the inhibitory effect of CNPs@DOX on the viability of 4T1 cells was significantly greater than of DOX (Fig. 3A). When the drug concentration was 10 mg/l, the inhibitory effect of CNPs@DOX on the viability of MCF7 cells was markedly greater than that of DOX (Fig. 3B). Nanomaterials have shown great potential in encapsulating and transporting drugs within tumor cells, penetrating cell membranes and releasing drugs via EPR effects (25), increasing drug accumulation within tumor cells but decreasing drug accumulation in normal cells (26). Therefore, CNPs@DOX, as a nanomaterial, may accelerate the internalization of drugs by cells, causing DOX to act on nuclei faster and kill tumor cells more effectively (27,28).

Cell apoptosis. The cytotoxic effects of DOX on tumor cells are mainly exerted via two mechanisms (29): One is to

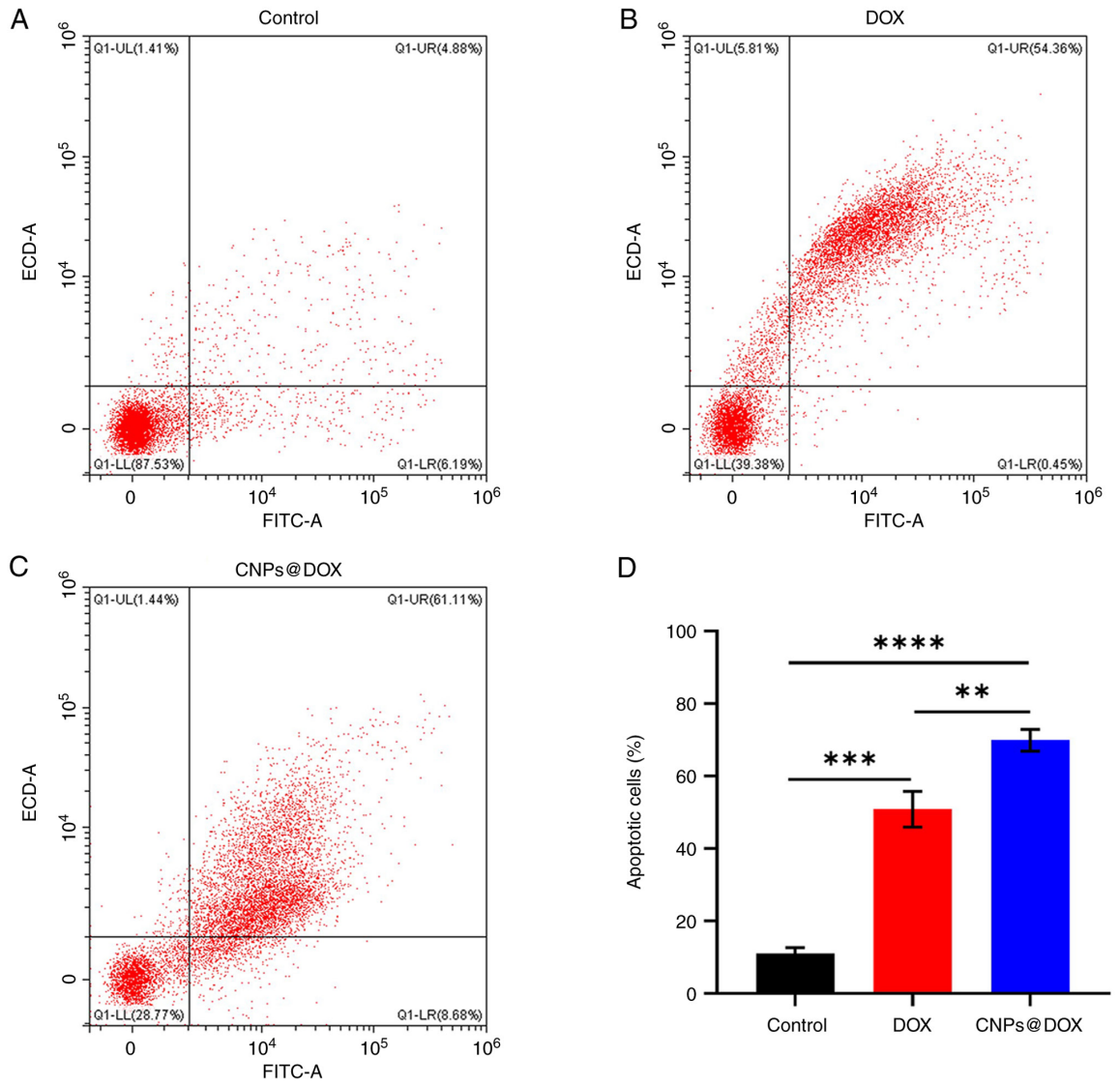

Figure 4. Cell apoptosis. Analysis of the apoptosis of 4T1 cells after different treatments for 24 h: (A) Control, (B) DOX (5 mg/l) and (C) CNPs@DOX (5 mg/l). The upper left quadrant represents cell debris due to mechanical damage; the lower left quadrant indicates normal cells; the upper right quadrant indicates late apoptotic cells; and the lower right quadrant indicates early apoptotic cells. (D) Quantification of the percentage of apoptotic 4T1 cells after different treatments. **P<0.01; ***P<0.001; ****P<0.0001. CNP, carbon nanoparticle; DOX, doxorubicin.

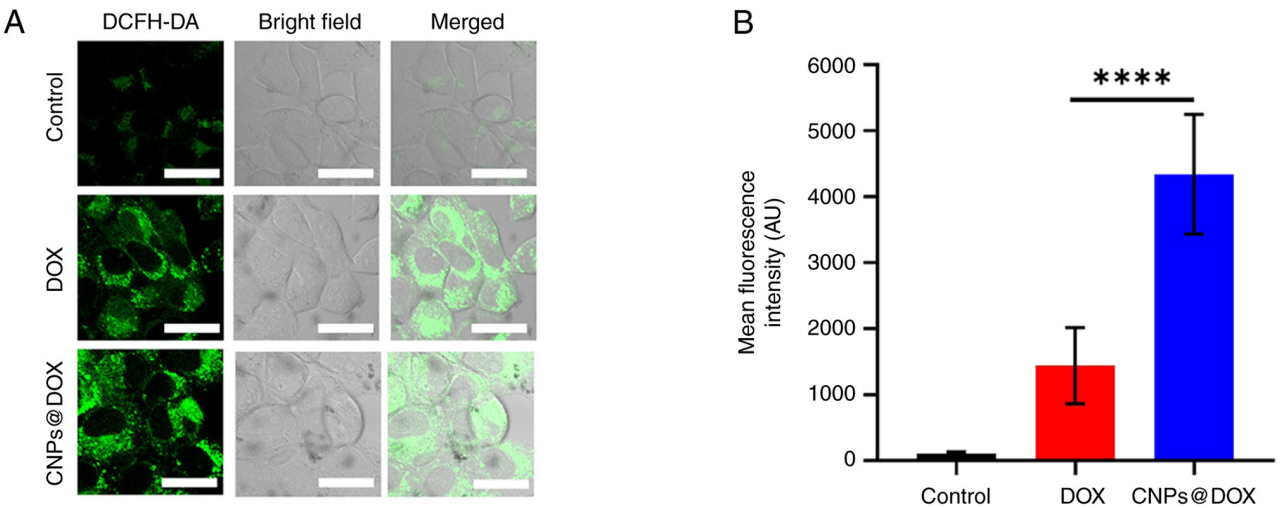

Figure 5. Intracellular ROS assay. (A) Fluorescence images of ROS produced after different treatments of 4T1 cells by confocal laser scanning microscopy. Scale bar, 20 μm. (B) Semi-quantitative fluorescence analysis of ROS produced. ****P<0.0001. ROS, reactive oxygen species; CNPs, carbon nanoparticles; DOX, doxorubicin, DCFH-DA, 2',7'-Dichlorodihydrofluorescein diacetate.

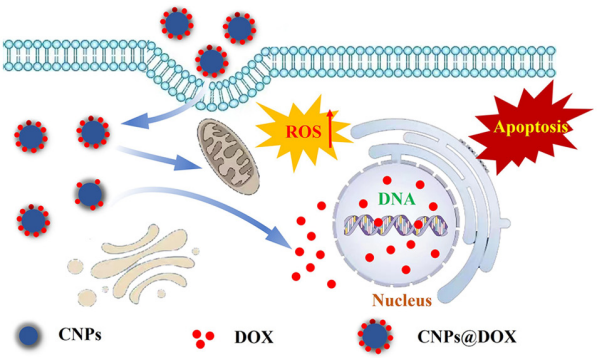

Figure 6. Schematic illustration of cell apoptosis induction by CNPs@DOX. CNPs, carbon nanoparticles; DOX, doxorubicin; ROS, reactive oxygen species.

insert G-C base pairs into the DNA sequence to induce cell apoptosis by inhibiting DNA replication (30); and the other is that DOX acts as an electron acceptor in the redox reaction and is oxidized into semi-quinone free radicals, which causes oxidative damage to cell membranes, protein and DNA through the generation of ROS, thus inducing the apoptosis of cancer cells (31). The present study evaluated the effect of CNPs@DOX and DOX on the apoptosis of 4T1 cells. The results demonstrated that the rates of apoptosis of 4T1 cells in the DOX and CNPs@DOX groups were 50.85±4.91 and 69.89±2.99%, respectively, which were significantly higher than the rate of 11.02±1.64% in the control group (Fig. 4). In addition, the apoptosis rate of the CNPs@DOX group was also significantly higher than that of DOX group, indicating that CNPs@DOX significantly increased the apoptosis of the 4T1 cells, and the drugs delivered by CNPs could serve an antitumor role by promoting cell apoptosis.

Intracellular ROS assay. ROS are metabolic by-products of cellular aerobic respiration and serve an important role in cell signaling and homeostasis (32). Different ROS control diverse aspects of cell behavior from signaling to death, and dysregulation of ROS production and ROS limitation pathways are common features of cancer cells (33). Previous studies have reported that chemotherapy drugs can promote apoptosis and inhibit tumor growth by increasing ROS levels in tumor cells (34,35). The present study used the DCFH-DA fluorescent probe to detect intracellular ROS production and CLSM to detect DCF fluorescence to determine intracellular ROS levels. The results demonstrated that green fluorescence was notably enhanced after the 4T1 cells were incubated with DOX and CNPs@DOX, whilst almost no green fluorescence was detected in the control group (Fig. 5A). In addition, semi-quantitative fluorescence results further indicated that the amount of ROS produced in the CNPs@DOX group was significantly higher than that in the DOX group (Fig. 5B). These results indicate that CNPs@DOX can increase intracellular ROS levels, thereby promoting tumor cell apoptosis and inhibiting tumor growth.

Limitations. The present study only demonstrated that CNPs@DOX had a good killing effect on tumor cells at the cellular level and failed to carry out experiments at the animal level to further explore the anti-tumor effect of CNPs@DOX, which is the limitation of this study.

Conclusion. The present study used CNPs as a nanocarrier for DOX to prepare a novel nanomedicine delivery system, CNPs@DOX (Fig. 6). Through UV-vis and fluorescence spectrophotometry, ζ potential and TEM characterization experiments, the results obtained indicated that the nano-drug delivery system CNPs@DOX, with a drug loading rate of 77.52% and particle size of 96±17 nm, was successfully prepared. Furthermore, *in vitro* experiments demonstrated that CNPs@DOX could promote tumor cell apoptosis by increasing intracellular ROS levels, which should have good antitumor effects and great clinical application potential in tumor therapy.

Acknowledgements

Not applicable.

Funding

The present study was supported by the National Natural Science Foundation of China (grant nos. 82104629, 8200410 and 82305034), the Natural Science Foundation of Guangdong Province (grant nos. 2021A1515010673 a nd 2023A1515011078), the Traditional Chinese Medicine Administration Project of Guangdong Province (grant nos. 20231389 and 20221256), the Science and Technology Program of Yangjiang (grant nos. SF2021049, SF2022001, SF2023026 and SF2023027) and the Scientific Research Fund of Yangjiang People's Hospital (grant nos. 2021003, G2021002 and G2021004).

Availability of data and materials

The data generated in the present study may be requested from the corresponding author.

Authors' contributions

YLi and JZ wrote the original draft of the manuscript, and created figures, tables and visual representations of the data. CW, YLa, HF and QW analyzed and interpreted the data. YLi, JZ and XJ conceived and designed the study. ZL, JC and XZ performed the experiments. YLi, JZ and XJ confirm the authenticity of all the raw data. All authors have read and approved the final manuscript.

Ethics approval and consent to participate

Not applicable.

Patient consent for publication

Not applicable.

Competing interests

The authors declare that they have no competing interests.

References

1. Qi J, Li M, Wang L, Hu Y, Liu W, Long Z, Zhou Z, Yin P and Zhou M: National and subnational trends in cancer burden in China, 2005-20: An analysis of national mortality surveillance data. Lancet Public Health 8: e943-e955, 2023.
2. Sung H, Ferlay J, Siegel RL, Laversanne M, Soerjomataram I, Jemal A and Bray F: Global cancer statistics 2020: GLOBOCAN estimates of incidence and mortality worldwide for 36 cancers in 185 countries. CA Cancer J Clin 71: 209-249, 2021.
3. Cao W, Chen HD, Yu YW, Li N and Chen WQ: Changing profiles of cancer burden worldwide and in China: A secondary analysis of the global cancer statistics 2020. Chin Med J (Engl) 134: 783-791, 2021.
4. Lin L, Li Z, Yan L, Liu Y, Yang H and Li H: Global, regional, and national cancer incidence and death for 29 cancer groups in 2019 and trends analysis of the global cancer burden, 1990-2019. J Hematol Oncol 14: 197, 2021.
5. Zaimy MA, Saffarzadeh N, Mohammadi A, Pourghadamyari H, Izadi P, Sarli A, Moghaddam LK, Paschepari SR, Azizi H, Torkamandi S and Tavakkoly-Bazzaz J: New methods in the diagnosis of cancer and gene therapy of cancer based on nanoparticles. Cancer Gene Ther 24: 233-243, 2017.
6. Cao J, Huang D and Peppas NA: Advanced engineered nanoparticulate platforms to address key biological barriers for delivering chemotherapeutic agents to target sites. Adv Drug Deliv Rev 167: 170-188, 2020.
7. Williams HD, Trevaskis NL, Charman SA, Shanker RM, Charman WN, Pouton CW and Porter CJ: Strategies to address low drug solubility in discovery and development. Pharmacol Rev 65: 315-499, 2013.
8. Tang L, Jiang W, Wu L, Yu X, He Z, Shan W, Fu L, Zhang Z and Zhao Y: TPGS2000-DOX prodrug micelles for improving breast cancer therapy. Int J Nanomedicine 16: 7875-7890, 2021.
9. Wu Y, Wang Z, Han L, Guo Z, Yan B, Guo L, Zhao H, Wei M, Hou N, Ye J, *et al*: PRMT5 regulates RNA m6A demethylation for doxorubicin sensitivity in breast cancer. Mol Ther 30: 2603-2617, 2022.
10. Etrych T, Daumová L, Pokorná E, Tušková D, Lidický O, Kolářová V, Pankrác J, Šefc L, Chytil P and Klener P: Effective doxorubicin-based nano-therapeutics for simultaneous malignant lymphoma treatment and lymphoma growth imaging. J Control Release 289: 44-55, 2018.
11. Yan D, Wei H, Lai X, Ge Y, Xu S, Meng J, Wen T, Liu J, Zhang W, Wang J and Xu H: Co-delivery of homoharringtonine and doxorubicin boosts therapeutic efficacy of refractory acute myeloid leukemia. J Control Release 327: 766-778, 2020.
12. Almajidi YQ, Kadhim MM, Alsaikhan F, Turki Jalil A, Hassan Sayyid N, Alexis Ramírez-Coronel A, Hassan Jawhar Z, Gupta J, Nabavi N, Yu W and Ertas YN: Doxorubicin-loaded micelles in tumor cell-specific chemotherapy. Environ Res 227: 115722, 2023.
13. Hong Y, Che S, Hui B, Yang Y, Wang X, Zhang X, Qiang Y and Ma H: Lung cancer therapy using doxorubicin and curcumin combination: Targeted prodrug based, pH sensitive nanomedicine. Biomed Pharmacother 112: 108614, 2019.
14. Zhu L and Lin M: The synthesis of nano-doxorubicin and its anticancer effect. Anticancer Agents Med Chem 21: 2466-2477, 2021.
15. Fernandez-Fernandez A, Manchanda R and McGoron AJ: Theranostic applications of nanomaterials in cancer: Drug delivery, image-guided therapy, and multifunctional platforms. Appl Biochem Biotechnol 165: 1628-1651, 2011.
16. Zhang J, Yin X, Li C, Yin X, Xue Q, Ding L, Ju J, Ma J, Zhu Y, Du D, *et al*: A Multifunctional Photoacoustic/Fluorescence Dual-Mode-Imaging Gold-Based Theranostic Nanoformulation without External Laser Limitations. Adv Mater 34: e2110690, 2022.
17. Patel SC, Lee S, Lalwani G, Suhrland C, Chowdhury SM and Sitharaman B: Graphene-based platforms for cancer therapeutics. Ther Deliv 7: 101-116, 2016.
18. Lin J, Chen X and Huang P: Graphene-based nanomaterials for bioimaging. Adv Drug Deliv Rev 105(Pt B): 242-254, 2016.
19. Zhao H, Ding R, Zhao X, Li Y, Qu L, Pei H, Yildirimer L, Wu Z and Zhang W: Graphene-based nanomaterials for drug and/or gene delivery, bioimaging, and tissue engineering. Drug Discov Today 22: 1302-1317, 2017.
20. Díez-Pascual AM: Carbon-Based Nanomaterials. Int J Mol Sci 22: 7726, 2021.
21. Oh B and Lee CH: Development of thiolated-graphene quantum dots for regulation of ROS in macrophages. Pharm Res 33: 2736-2747, 2016.
22. Zhang J, Chen L, Shen B, Chen L, Mo J and Feng J: Dual-Sensitive graphene oxide loaded with proapoptotic peptides and anticancer drugs for cancer synergetic therapy. Langmuir 35: 6120-6128, 2019.
23. Sharifi S, Behzadi S, Laurent S, Forrest ML, Stroeve P and Mahmoudi M: Toxicity of nanomaterials. Chem Soc Rev 41: 2323-2343, 2012.
24. Guan M, Li J, Jia Q, Ge J, Chen D, Zhou Y, Wang P, Zou T, Zhen M, Wang C and Shu C: A versatile and clearable nanocarbon theranostic based on carbon dots and gadolinium metallofullerene nanocrystals. Adv Healthc Mater 5: 2283-2294, 2016.
25. Peer D, Karp JM, Hong S, Farokhzad OC, Margalit R and Langer R: Nanocarriers as an emerging platform for cancer therapy. Nat Nanotechnol 2: 751-760, 2007.
26. Yuan Y, Cai T, Xia X, Zhang R, Chiba P and Cai Y: Nanoparticle delivery of anticancer drugs overcomes multidrug resistance in breast cancer. Drug Deliv 23: 3350-3357, 2016.
27. Donahue ND, Acar H and Wilhelm S: Concepts of nanoparticle cellular uptake, intracellular trafficking, and kinetics in nanomedicine. Adv Drug Deliv Rev 143: 68-96, 2019.
28. Li R, Wang Y, Du J, Wang X, Duan A, Gao R, Liu J and Li B: Graphene oxide loaded with tumor-targeted peptide and anti-cancer drugs for cancer target therapy. Sci Rep 11: 1725, 2021.
29. Cagel M, Grotz E, Bernabeu E, Moretton MA and Chiappetta DA: Doxorubicin: Nanotechnological overviews from bench to bedside. Drug Discov Today 22: 270-281, 2017.
30. Thorn CF, Oshiro C, Marsh S, Hernandez-Boussard T, McLeod H, Klein TE and Altman RB: Doxorubicin pathways: Pharmacodynamics and adverse effects. Pharmacogenet Genomics 21: 440-446, 2011.
31. Chen K, Cai H. Zhang H, Zhu H, Gu Z, Gong Q and Luo K: Stimuli-responsive polymer-doxorubicin conjugate: Antitumor mechanism and potential as nano-prodrug. Acta Biomater 84: 339-355, 2019.
32. Dharmaraja AT: Role of reactive oxygen species (ROS) in therapeutics and drug resistance in cancer and bacteria. J Med Chem 60: 3221-3240, 2017.
33. Cheung EC and Vousden KH: The role of ROS in tumour development and progression. Nat Rev Cancer 22: 280-297, 2022.
34. Sp N, Kang DY, Jo ES, Rugamba A, Kim WS, Park YM, Hwang DY, Yoo JS, Liu Q, Jang KJ and Yang YM: Tannic Acid Promotes TRAIL-Induced extrinsic apoptosis by regulating mitochondrial ROS in human embryonic carcinoma cells. Cells 9: 282, 2020.
35. Yao W, Lin Z, Shi P, Chen B, Wang G, Huang J, Sui Y, Liu Q, Li S, Lin X, *et al*: Delicaflavone induces ROS-mediated apoptosis and inhibits PI3K/AKT/mTOR and Ras/MEK/Erk signaling pathways in colorectal cancer cells. Biochem Pharmacol 171: 113680, 2020.